How Do Conservation Laws Define A Motion Suppression Score In In-vivo Ivus Sequences?

Aura Hernàndez[1], Debora Gil[1] and Albert Teis[2]

[1]Computer Vision Center, Edifici O, Universitat Autònoma de Barcelona, Bellaterra, Spain
[2]Hospital Universitari "Germans Trias i Pujol", Badalona, Spain

***Abstract*— Evaluation of arterial tissue biomechanics for diagnosis and treatment of cardiovascular diseases is an active research field in the biomedical imaging processing area. IntraVascular UltraSound (IVUS) is a unique tool for such assessment since it reflects tissue morphology and deformation. A proper quantification and visualization of both properties is hindered by vessel structures misalignments introduced by cardiac dynamics. This has encouraged development of IVUS motion compensation techniques. However, there is a lack of an objective evaluation of motion reduction ensuring a reliable clinical application This work reports a novel score, the Conservation of Density Rate (CDR), for validation of motion compensation in *in-vivo* pullbacks. Synthetic experiments validate the proposed score as measure of motion parameters accuracy; while results in *in vivo* pullbacks show its reliability in clinical cases.**

***Keywords*: validation standards, IVUS motion compensation, conservation laws.**

I. Introduction

Clinical effectiveness of intravascular treatments (such as stent placement [1] or atherosclerotic disease assessment [2]) depend, among other factors, on tissue biomechanical properties. Arterial tissue elastic properties, and detection of rupture-prone vulnerable plaques, in particular, are one of the most active areas of research in both the cardiology and biomedical imaging communities [1], [2], [3], [4]. Determination of the main mechanical properties, currently under study, requires exploring vessel tissue deformation along the cardiac cycle. By their capability of reflecting vessel morphology and dynamics, IntraVascular UltraSound sequences represent a unique tool for the evaluation of tissue mechanical properties. Unfortunately, cardiac dynamics introduce a misalignment of vessel structures in images as well as a saw-tooth-shape in the longitudinal view appearance of vessel borders that hinders visualization, accuracy of volumetric measures and evaluation of tissue deformation [5]. This has motivated, in the last years, the development of several IVUS in-plane motion compensation techniques [6], [7], [8], [9].

In order to ensure a high applicability in clinical practice, special care should be taken in defining an objective measure allowing assessment of motion parameters accuracy in real data. In real pullbacks there is no objective error measure indicating the amount of motion suppressed, since motion parameters are unknown. In most cases, quality measures are either subjective measures, based on the visual appearance of sequences and longitudinal cuts [6], [9] or rely on extraction of vessel properties (such as strain in [7]). We consider that such an important issue as the validation protocol deserves special attention.

This work reports a novel score, the Conservation of Density Rate (CDR), for validation of motion compensation in in-vivo pullbacks. Basing on fluid mechanics conservation laws [10] we consider the changes that the local density of mass (given by the image local mean) experiences along the sequence. The more aligned the sequence is, the less variability the local density presents. The ratio between the amplitudes of the Fourier coefficient corresponding to the cardiac frequency before and after image alignment reflects, for each pixel, the local reduction in cardiac motion [11]. We account for any motion artifact introduced by the correcting algorithm by adding a factor measuring the conservation of the total mass. We define the CDR score as the trimmed mean for the upper percentile of the local reduction score so that only pixels where motion is noticeable are taken into account. Two different sets of tests are presented: assessment on phantom sequences and performance on real pullbacks. Phantoms serve to assess the ability of CDR to quantify the misalignment rate, while in-vivo pullbacks show the correlation to the visual appearance of longitudinal cuts.

The remains of the paper are structured as follows. Section II is devoted to the definition of the quality measure. Experiments on phantom and real sequences, including a clinical application, are reported in Section III. Discussions and conclusions are detailed in Section IV.

II. Defining a Score for Cardiac Rigid Motion Compensation

Any comparative quantity reflecting image changes along a sequence, captures, in the case of IVUS, differences in morphology as well as vessel misalignments. Since after motion correction, vessel morphological changes still remain, only dynamic components should be considered.

Since vessel dynamics is mainly induced by cardiac motion, we use the Fourier transform for comparing cardiac terms. Let $\widehat{CQ}_0$, $\widehat{CQ}_1$ be the Fourier developments of any comparative quantity before and after motion correction and consider the principal cardiac frequency, namely ω_c. We define the Cardiac

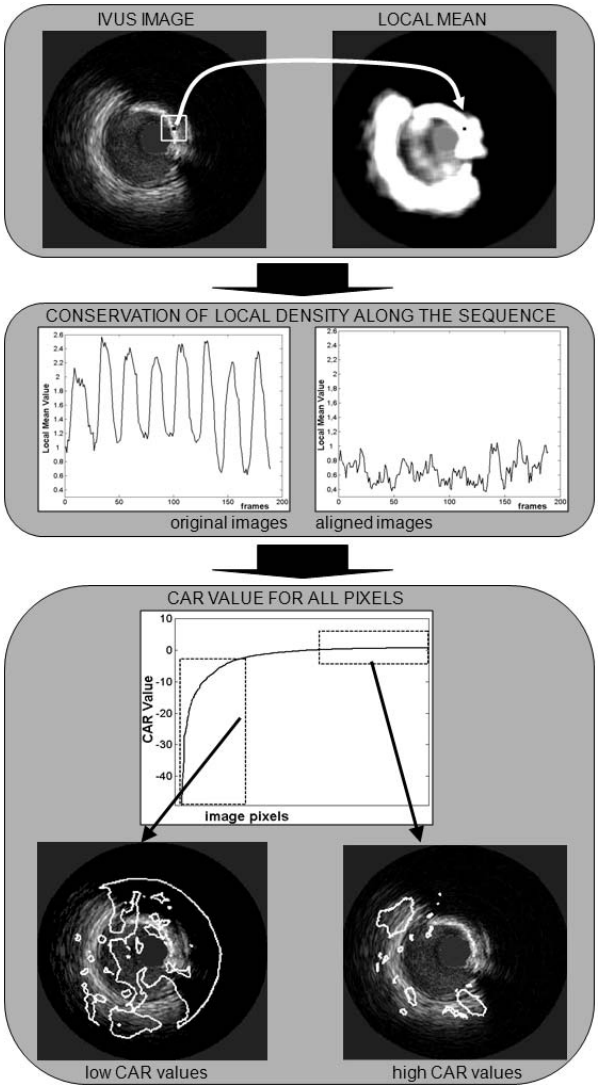

Fig. 1. Quality Measure Computation

Alignment Rate (*CAR*) as:

$$CAR := 1 - \frac{|\widehat{CQ}_1(\omega_c)|}{|\widehat{CQ}_0(\omega_c)|} \frac{\sum_{\omega \notin \Omega_c} |\widehat{CQ}_1|}{\sum_{\omega \notin \Omega_c} |\widehat{CQ}_0|}$$

The interval $\Omega_c = [\omega_c, 3\omega_c]$ defines the range of frequencies associated to cardiac motion. The second factor accounts for any motion artifacts introduced in the processed sequences. The *CAR* index equals 1 in the case that all cardiac motion has been suppressed, while approaches zero (or becomes even negative) for a poor rate of motion reduction.

Vessel motion is not visually noticed at all image pixels but only at some salient areas, such as calcium transitions. This motivates adopting a local approach and tracking image motion for each pixel. Usual similarity measures compare images in the framework of integrable functions [12] and are prone to give less reliable outputs if they are computed on small sets of pixels. Inspired on the strategies used in classic fluid mechanics [10], we propose exploring the conservation of a physical quantity along the sequence. In particular, we have chosen the local density of mass, since it will remain constant along the sequence in the measure that vessel structures are aligned. By the ultrasound properties, the image grey-values are proportional to the density of mass of tissue. We approximate the tissue local density by the image local mean computed in sliding windows 9×9 pixels large. The values of the local mean for all images provide each pixel with a function that describes the conservation of the local density of mass along the sequence. The *CAR* score for each of these functions provides a measure of the amount of local motion around each pixel.

Figure 1 sketches the main steps involved in the computation of the CAR index: computation of the image descriptor (upper block), conservation of local density along the sequence for a given pixel (middle block) and the *CAR* value for all pixels (bottom block). The first block illustrates the modeling of the local density of mass in terms of the image local mean. The local mean of the image (shown on the right) is obtained by computing, for each pixel, the image mean on a window (white square on the left image) centered on each pixel (black point). In the second block of the figure, we have the evolution of the local mean at a single pixel before (plot on the left) and after (plot on the right) image alignment. The plot obtained before alignment presents a well defined periodic behavior; afterwards, although the periodic pattern has been suppressed, the function still presents a variability due to noise and morphologic changes. The third block shows the *CAR* values obtained for all image pixels. The top plot shows the sorted *CAR* values and the bottom images show the position on the image of pixels achieving extreme values (dotted squares on the *CAR* plot). Since rigid motion is a global phenomenon, all pixels should present a similar value. However at blood and outer areas (not belonging to vessel structures), since motion is not noticeable, the reduction score achieves extreme low values (left bottom image). This motivates considering the *CAR* upper percentiles. In fact, we have that the sorted *CAR* values (top plot) asymptotically converge towards the true motion reduction rate.

We define our Conservation of Density Rate (*CDR*) as the trimmed mean [13] of the *CAR* value computed for the image local average:

$$CDR := \mu(\{CAR \mid CAR > prct\}) \qquad (1)$$

for $prct$ a given percentile. The *CDR* score, as well as any error, can be regarded as a random variable. In this framework, we have empirically proved (see experiments on phantoms in sect. III-A) that the *CDR* computed for the superior 55% percentile statistically correlates to the rotation relative error.

III. CDR Assessment

A. Phantom Data

Our synthetic experiments focus on addressing the reliability of *CDR* as measure of motion compensation. Phantoms have been generated by applying a motion pattern to a block of IVUS images representing a still artery pullback. The still vessel images have been obtained by compensating motion of an *in vivo* pullback. Motion patterns have been extracted from parameters estimated from 5 test sequences. The algorithm

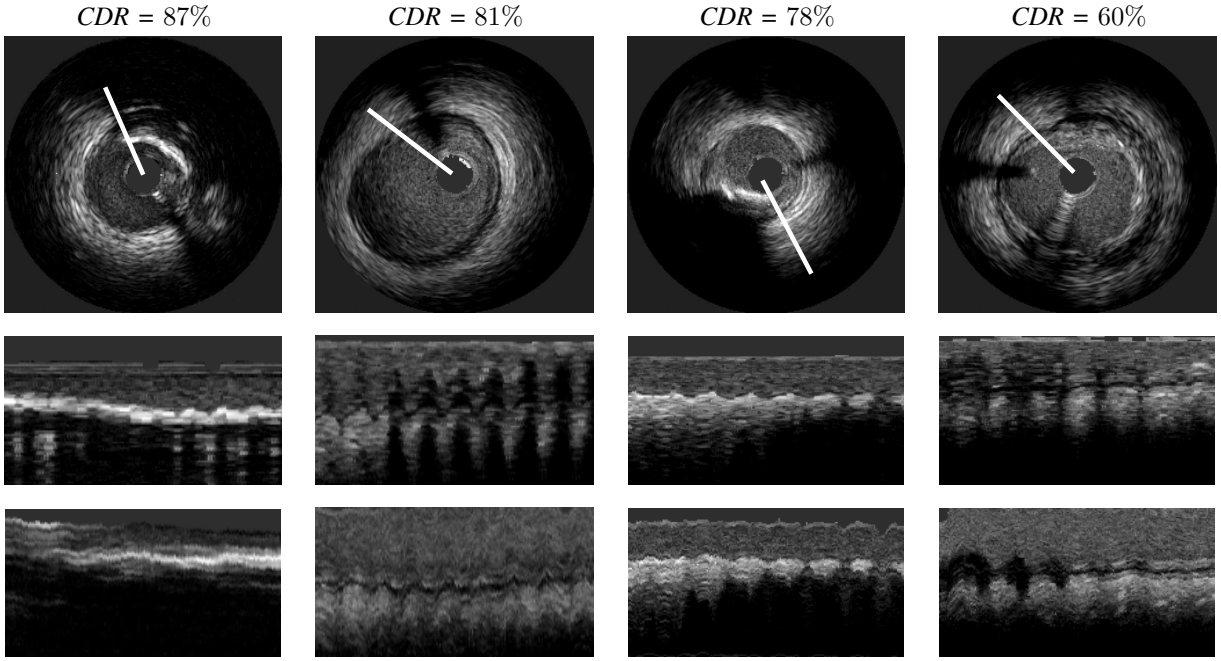

Fig. 2. Longitudinal cuts. Each column corresponds to each patient, from the best *CDR* to the worst one.

used to compute IVUS motion is the one described in [8], which considers compensation of in-plane rigid motion. In order to check whether *CDR* detects motion artifacts introduced by the correcting algorithm, we have added a random rotation to the estimated motions.

The average ($\|\cdot\|_1$ norm) of the relative error is our quality measure for each phantom and its statistical range (given by the mean $\pm$ the variance) reports the performance for all cases. In order to validate the quality measure we have compared *CDR* values to the rotation angle relative accuracy (in $\%$) given by 1 minus its relative error. Student T-tests and confidence intervals (at 95% of confidence) are used to check whether there is any significant difference between means.

TABLE I
CDR CORRELATION TO MOTION COMPENSATION

	Sequence	Random
REL. ACC.	74.5 $\pm$ 13.3	67.6 $\pm$ 13.8
CDR	74.4 $\pm$ 9.8	70.0 $\pm$ 11.3
p-val	0.9995	0.9500
CI	(-7.8, 7.7)	(-9.5,9.0)

Table I reports the statistics summary for the validation of *CDR* as accuracy score. We report, for both phantoms, ranges for the angle relative accuracy (REL. ACC.) and *CDR*, as well as, the T-test p-value and the confidence interval (CI) for the difference in means. There is no significance difference between *CDR* and relative accuracy with at most a discrepancy between -9.5% and 9.0%.

B. Experimental Data

Performance in real pullbacks has been validated by testing the proposed approach in 32 vessel segments (17 left anterior descending and 15 right coronary arteries) extracted from clinical cases of the Hospital Universitari "Germans Trias i Pujol" in Badalona, Spain. Sequences have been recorded using a Galaxy-BostonSci device at 40 MHz, constant pullback and a digitalization rate of 30 fps. The segments analyzed are short segments 5-6 mm long and cover different plaques (from soft to calcified), morphologies (including branches) and motion artifacts (such as longitudinal motion). Rigid motion was compensated using the approach described in [8].

Figure 2 shows four cases with decreasing *CDR* values (from left to right): 87%, 81%, 78% and 60%. The first row shows a frame of the original sequences, the second one the longitudinal cuts before motion compensation and the last row the cut after sequence alignment. In the first column (fig.2(a)) we show a sequence with structure misalignment. The calcium shadow appears and disappears in the original longitudinal cut due to rotation, while calcium presents a uniform appearance in the aligned cut. In the second column (fig.2(b)) we show a sequence presenting a noticeable vessel translation and its associated tooth-saw-shape in the original longitudinal cut (especially at the end of the segment). After motion correction, only a subtle undulation due to radial dilation (at the beginning of the cut) remains. The longitudinal cuts in fig.2(c) show a straight profile (both before and after alignment) in spite of a lower *CDR*. This phenomenon, which appears in the absence of motion, is inherent to any relative measure. Finally, in fig.2(d) we show the worst performer both in terms of longitudinal cut appearance and *CDR* value. In this last case, a proper alignment is only achieved at the second half of the segment and, those, we have only a 60% of motion reduction.

C. Clinical Potential

A clinical application of the method is tracking continuous vessel structures, such as vessel walls. Stabilized sequences

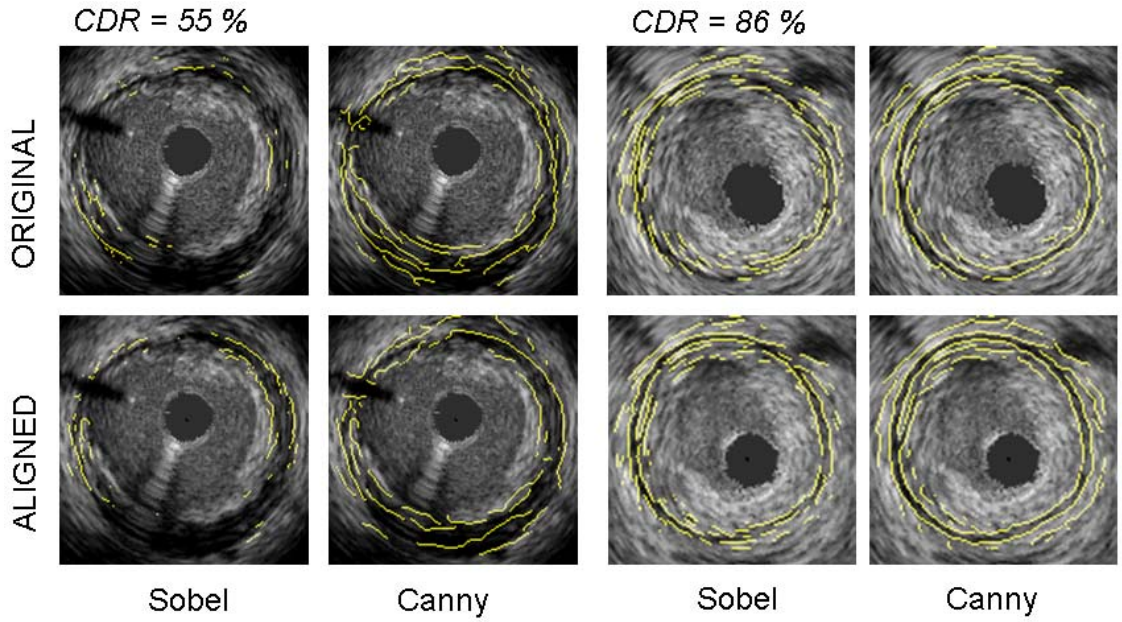

Fig. 3. Vessel External Wall Alignment for a low (left images) and high (right images) *CDR*.

preserve the local density of mass of structures along the time, so a mean of the sequence enhances those structures, while blurs texture and speckle. We have computed edges (using both Sobel and Canny detectors) on average of stabilized and non-stabilized sequences for a low and high *CDR*.

Figure 3 shows the edges (yellow lines) around the vessel external wall for $CDR = 50\%$ (left images) and $CDR = 86\%$ (right images). In the case of a high *CDR* both Canny and Sobel give continuous profiles of the vessel external wall for aligned sequences. For a low *CDR*, although stabilized sequences give more continuous contours, they fail to provide closed curves.

IV. Conclusions

This paper approaches assessment of artery motion compensation in IVUS sequences. We address the definition of an objective score (*CDR*) measuring motion reduction in experimental data. We present experiments on synthetic sequences (phantoms) and *in vivo* pullbacks and also a clinical application.

Performance on phantom sequences (table I) shows that *CDR* statistically compares to the relative accuracy in parameter estimation, which validates it as a motion suppression measure. Results on real pullbacks show that a high *CDR* guarantees a straight profile of longitudinal cuts. We also show its clinical usefulness by improving the detection and tracking of vessel structures.

By the former considerations we conclude that the *CDR* score is an objective measure of image alignment in experimental data which correlates to parameters accuracy and longitudinal cuts appearance. The fact that its computation relies exclusively on image local appearance evolution validates the *CDR* score as experimental measure of image alignment.

Acknowledgments

This work was supported by the Spanish Government FIS projects PI070454 and PI071188. The second author is supported by The Ramón y Cajal Program.

References

[1] J. Wentzel and R. K. et al, "Relationship between neointimal thickness and shear stress after wallstent implantation in human coronary arteries," *Circulation*, vol. 103, no. 13, pp. 1740–5, 2001.

[2] J. Garcia, A. Crespo, J. Goicolea, M. Sanmartin, and C. Garcia, "Study of the evolution of the shear stress on the restenosis after coronary angioplasty," *Journal of Biomechanics*, vol. 39, no. 5, pp. 799–805, 2006.

[3] I. A. Kakadiaris, S. M. O'Malley, M. Vavuranakis, S. Carlier, R. Metcalfe, C. J. Hartley, E. Falk, and M. Naghavi, "Signal-processing approaches to risk assessment in coronary artery disease," Department of Computer Science, University of Houston, Tech. Rep. UH-CS-06-09, June 2006.

[4] E. Céspedes, C. Korte, and A. van der Steen, "Intraluminal ultrasonic palpation: assessment of local cross-sectional tissue stiffness," *Ultrasound Med. Biol.*, vol. 26, pp. 385–396, March 2000.

[5] P. Delachartre, C. Cachard, G. Finet, F. Gerfault, and D.Vray, "Modeling geometric artefacts in intravascular ultrasound imaging," *Ultrasound Med Biol*, vol. 25, no. 4, pp. 567–575, 1999.

[6] S. A. de Winter, R. Hamers, M. Degertekin, *et al.*, "Retrospective image-based gating of intracoronary ultrasound images for improved quantitative analysis: The intelligate method," *Catheterization and Cardiovascular Interv*, vol. 61, pp. 84–94, 2004.

[7] K. Y. E. Leung, R. Baldewsing, F. Mastik, and et al., "Motion compensation for intravascular ultrasound palpography for in vivo vulnerable plaque detection," in *IEEE Ultrasonics Symposium*, vol. 1, 2005, pp. 253– 256.

[8] A. Hernàndez, P. Radeva, A. Tovar, and D. Gil, "Vessel structures alignment by spectral analysis of ivus sequences," in *Proc. of CVII, MICCAI Workshop*, 2006.

[9] M. Rosales, P. Radeva, O. Rodriguez, and D. Gil, "Suppression of IVUS image rotation. a kinematic approach," in *FIMH*, vol. 3504, 2005, pp. 359–368.

[10] S. Whitaker, *Introduction to Fluid Mechanics*. Krieger Pub Co, 1992.

[11] D. Gil, O. Rodriguez-Leor, P. Radeva, and A. Hernàndez, "Assessing artery motion compensation in ivus," in *CAIP07*, 2007.

[12] W. Rudin, *Complex and Real Analysis*. McGraw-Hill Int. Ed., 1987.

[13] P. Rousseeuw and A. Leroy, *Robust Regression and Outlier Detection*. John Wiley and Sons, 1987.